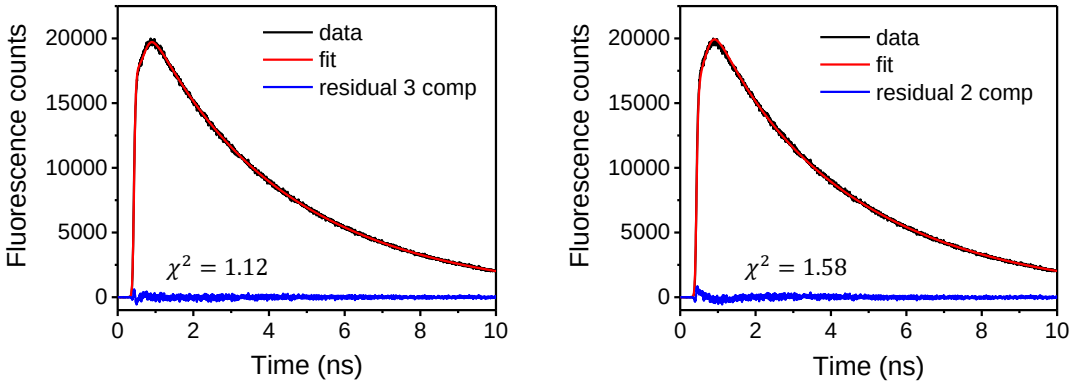

Figure S1. Time-resolved fluorescence experiments on CP29 WT (related to Table 1). Measured (in black) and fitted (in red) fluorescence time traces at 680 nm for CP29 WT upon 468 nm excitation. The difference between measured and fitted data (residuals) is displayed in blue. The left panel shows the 3-component fitting presented in the main text with the relative χ^2. The right panel shows a 2 component fitting for comparison (corresponding to a 84% component of 3.99 ns lifetime and a 16% component with 1.04 lifetime). A 3-component fitting results in significantly lower χ^2 and less structured residuals, implying that 3 components are necessary for a satisfactory fitting.

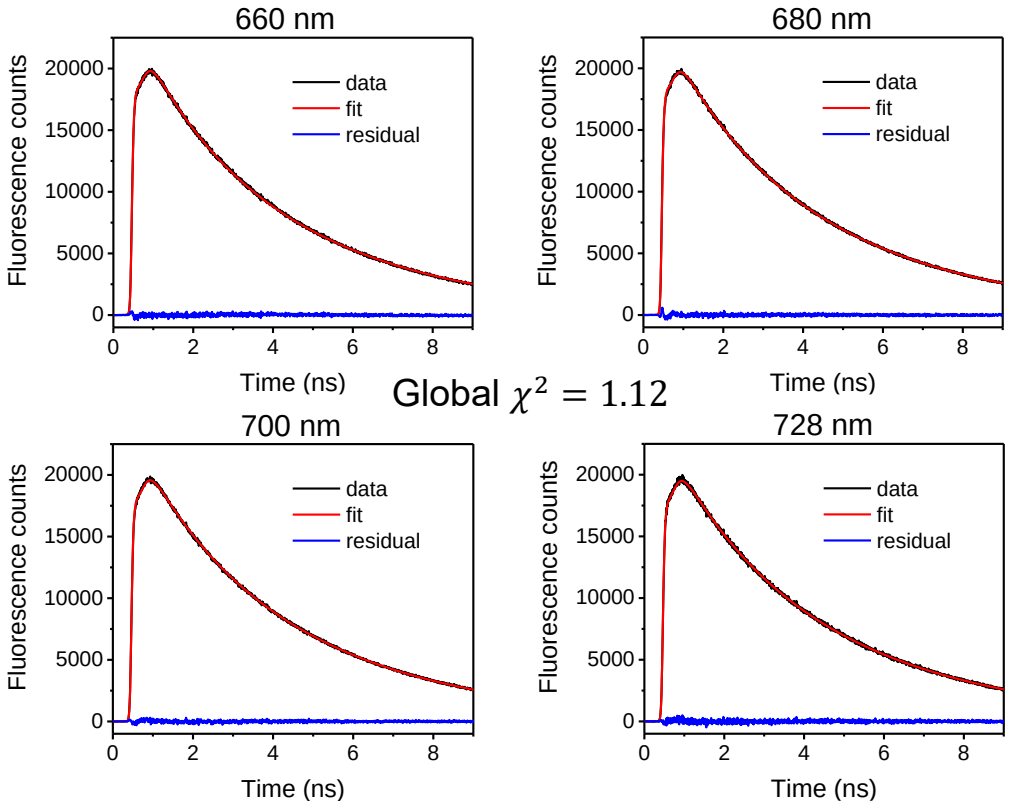

Figure S2. Time-resolved fluorescence experiments on CP29 WT at multiple wavelengths (related to Figure 2). Measured (in black) and fitted (in red) fluorescence time traces at selected wavelengths for CP29 WT upon 468 nm excitation. Residuals are displayed in blue.

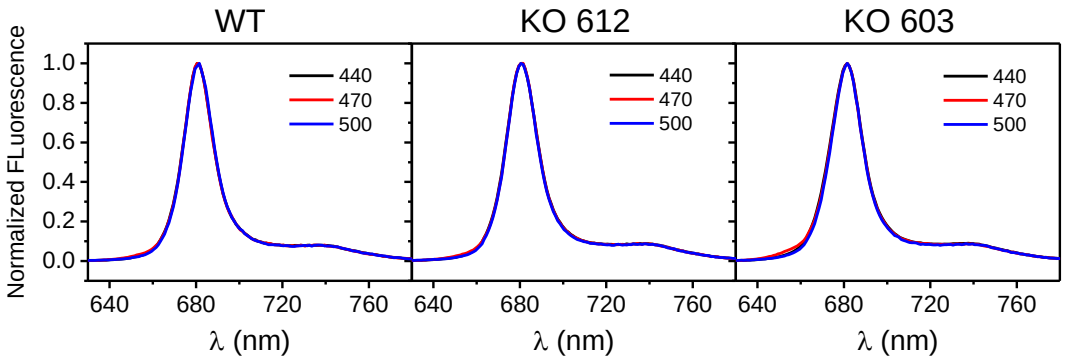

Figure S3. Steady-state fluorescence experiments. Steady-state fluorescence spectra of CP29 WT (left), KO612 (middle) and KO603 (right) for preferential chlorophyll a (440 nm, black line), chlorophyll b (470 nm, red line) and carotenoid (500 nm, blue line) excitation. The emission spectra of CP29 WT and KO603 peak at 681.5 nm, that of CP29 KO612 at 681 nm.

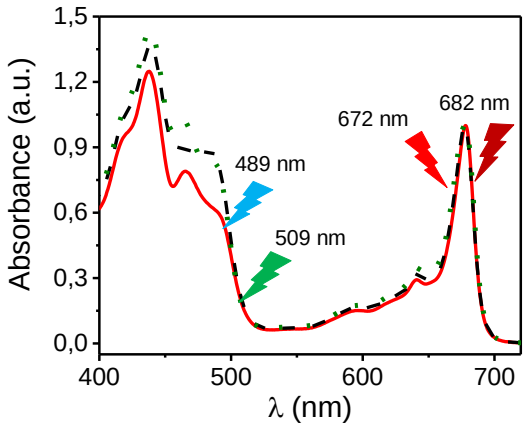

Figure S4. Steady-state absorption experiments. Absorption spectra of CP29 WT (red solid line), KO612 (black dashed) and KO603 (green dotted). The lightning bolts indicate the different excitation wavelengths for TA experiments (see methods in the main text).

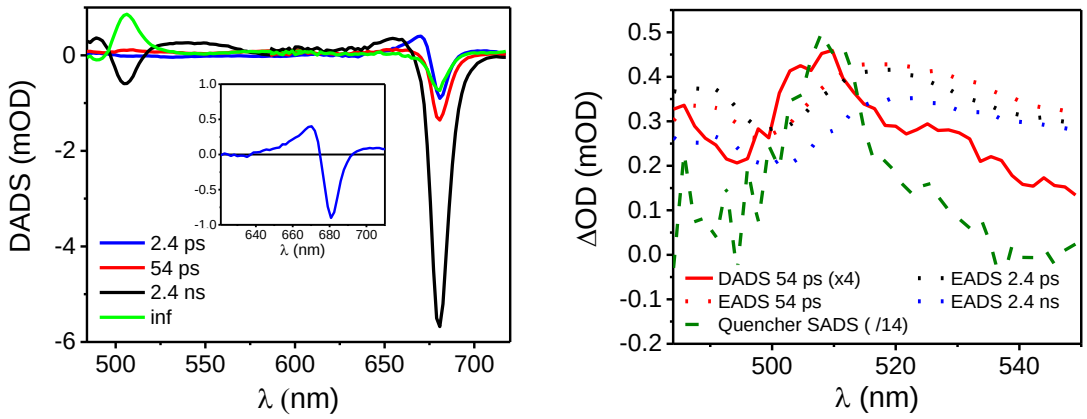

Figure S5. Global analysis of transient absorption experiments (related to Figure 3E-F). Left: DADS from global analysis of TA data upon 682 nm excitation of CP29 WT. The inset shows a magnification of the 2.4 ps DADS in the Qy region. Due to its bandshift feature, it can be assigned to a chlorophyll-chlorophyll uphill energy equilibration. Right: overlay of chlorophyll ESA profiles from 2.4 ps, 54 ps, and 2.4 ns EADS in Figure 3C-E of the manuscript (black, red and blue dotted lines) and the 54 ps DADS (multiplied by a factor of 4 for better comparison) from the DADS shown in the left panel. The quencher SADS as obtained from the heterogeneous target model presented in the main text is also shown for comparison (scaled by a factor of 14, green dashed line). The 54 ps DADS can be interpreted as a superposition of a typical chlrophyll spectrum with that of the quencher.

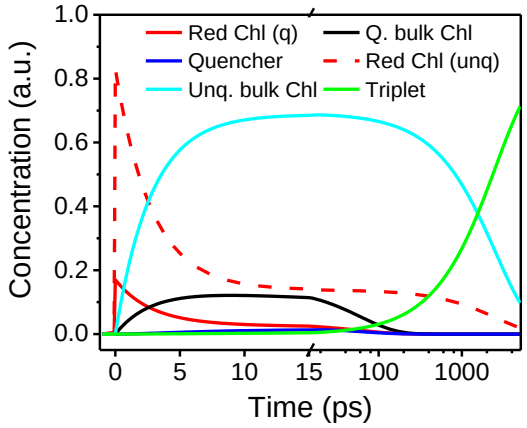

Figure S6. Results from the heterogeneous target model (related to Figure 4). Concentration profiles for the 6 species in the heterogeneous target model in the main text (see Figure 4A for the compartment kinetic model and Figure 4B for the SADS). Please note that the time axis is linear until 15 ps and logarithmic thereafter. The maximum of the quencher concentration is 0.013 at 20 ps. The same concentration profiles are also obtained for the above-mentioned alternative set of equality constraints, since the fitted kinetics are virtually unchanged.

Text S1. Details about the compartmental model and the equality constraints

As explained in the main text, the TA data for the 682 nm excitation experiment are modeled via a target compartmental scheme. The heterogeneity of the system is described by introducing two parallel schemes (each containing three compartments), representing unquenched/quenched complexes. More specifically, energy equilibration in the Qy region is described by an equilibrium between 2 pools of chlorophylls, a pre-equilibrated (red) pool representing the initial excitation of the 682 nm pulse and an equilibrated bulk pool. In order to simplify the kinetic modeling and reduce the number of free parameters, the spectra of the pre-equilibrated chlorophylls are assumed to be the same in the unquenched and quenched complexes. Both forward and backward rates of equilibration between red chlorophylls and bulk chlorophylls are also equated in quenched and unquenched CP29 (see arrows between red and black/cyan compartments in Figure 4A). These assumptions are justified by the evidence that the terminal emitter domain of quenched and unquenched complexes is unchanged (see also fluorescence data), suggesting that energy equilibration in the Qy is similar in both emissive states.

The weak signal in the chlorophyll Excited State Absorption (ESA) region required the use of equality constraints for the shapes of the chlorophyll SADS at wavelengths shorter than 630 nm. Different sets of constraints were therefore tested based on the same heterogeneous model schematized in Figure 4A of the main text. The main difference in these models is in the fitting quality in the region of chlorophyll ESA and in the shape of the resulting quencher spectrum, whereas the spectra of the triplet state and of all chlorophyll species in the Qy are insensitive to the different constraints. Due to the relatively low contribution of the signal in the chlorophyll ESA region to the overall residuals, the fitting quality was assessed not only by the total residual standard error, but also by visual inspection of the fitted and measured time traces. It is important to notice that all these models, despite some spectral changes, consistently result in a quencher SADS with typical features of a carotenoid excited state (i.e., a bleach below 500 nm and a positive difference absorption in the region between 500 and 560 nm).

The model which resulted in the best fitting quality (lower error and better reproduction of the signal in the chlorophyll ESA region, Figure S3) assumes that the ESA of red and bulk quenched chlorophylls (red and black compartments in Figure 4A) are equal, while the shapes of the ESA of unquenched bulk chlorophylls (cyan compartment) can differ slightly. The SADS for the described model are shown in Figure 4B (main text). A different set of equality constraints, where the ESA of quenched and unquenched chlorophylls are equated but can differ from that of red pre-equilibrated chlorophylls, gives almost identical result (data not shown). Another model, which equates the ESA profile of all chlorophyll species (red, black and cyan compartments in Figure 4A) yields a less satisfactory fitting, but it is shown below for completeness. The aforementioned equality constraints are more restrictive than those adopted in the model presented in the main text and, as a result, a lower fitting quality is achieved. As discussed previously, the fitting is not affected in the Qy region, where the largest part of the total signal is recorded. As a result, the kinetic rates are essentially the same as those obtained for the model shown in the main text (see Figure 4A). Moreover, the resulting fitting is, overall, almost as accurate as for the previous model (see Figure S7 and S8 for an overlay of fitted/measured data). However, even if the total residual error increases by only 0.5%, the fitting quality is significantly less satisfactory in the region between 530 nm and 560 nm (see Figure S9 to compare the different fitting qualities in this region). This new set of constraints also results in a different quencher spectrum (Figure S10), with a broad positive signal peaking around 530 nm and a strong bleach below 500 nm. This spectrum is significantly red-shifted and broader compared to the quencher spectrum shown in the main text but preserves typical features of a carotenoid singlet excited state. The peak position is also closer to the region where S_1 ESA is expected (see Figure 4C in the main text). However, the quencher spectrum is still blue-shifted compared to the CP29-bound lutein S_1 ESA spectrum (whose peak should be around 550 nm as previously measured[46]) and, even compared to the S_1 ESA spectrum of violaxanthin, it is broader and exhibits significantly more amplitude in the region at shorter wavelengths than the main peak. This evidence supports again the hypothesis that the quencher can be assigned to a carotenoid S* state. Anyway, the quencher spectrum going below zero above 570 nm and the lower fitting quality make this model less realistic than the one shown in the main text.

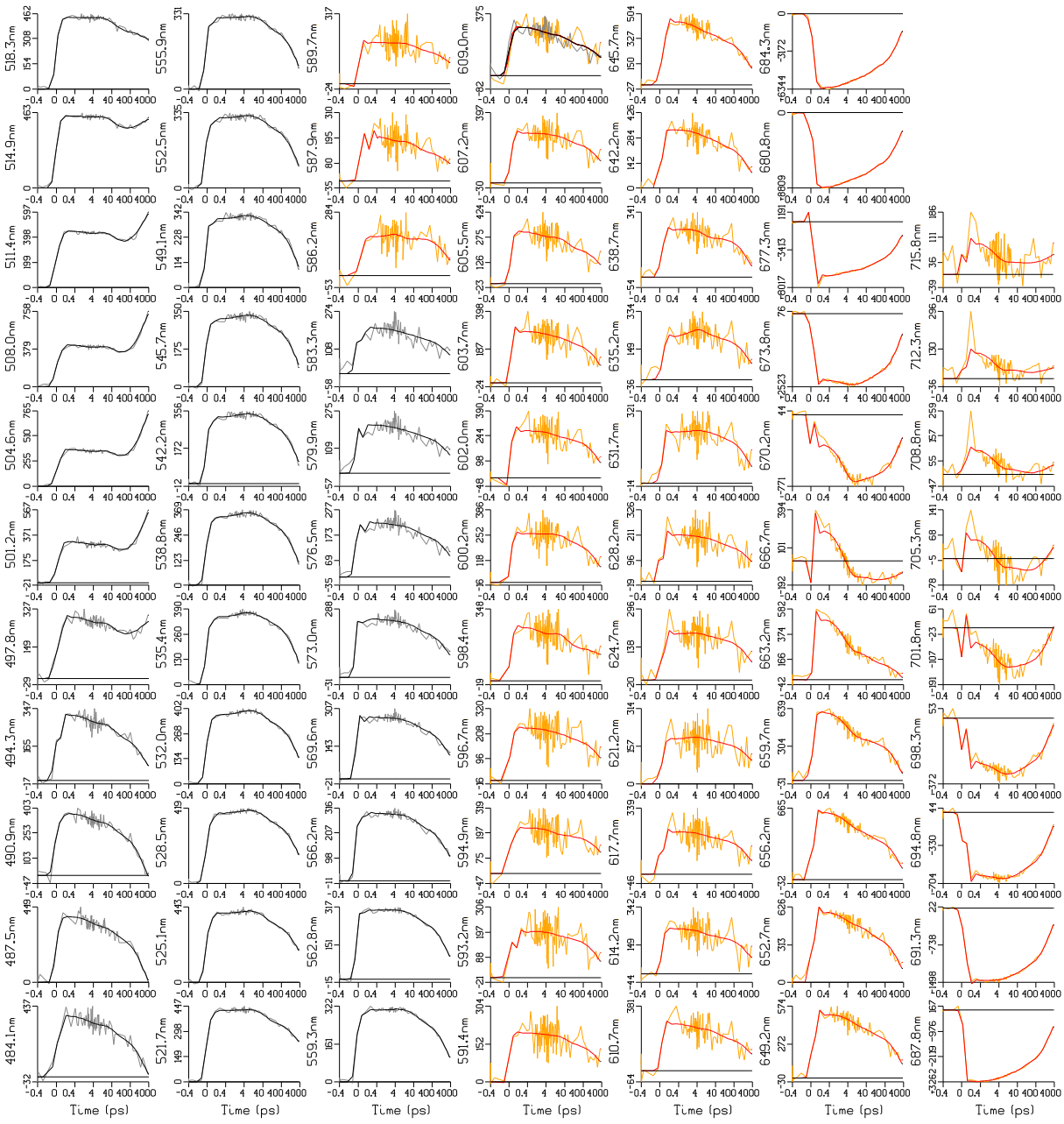

Figure S7. Transient absorption data and fitting (related to Figure 3). Time traces of raw data (light colors, in µOD) and fit (dark colors) with the equality constraints adopted in the main text (ESA profile of bulk unquenched chlorophyll compartment different from ESA profiles of other chlorophyll compartments). This is also the fitting yielding the best fit quality. Wavelength is indicated in the ordinate label of each panel. Please note that the time scale is linear until 0.4 ps and logarithmic thereafter. Please note that each panel is scaled to its maximum and all the time zeroes (location of the maximum of the IRF) are chirp corrected.

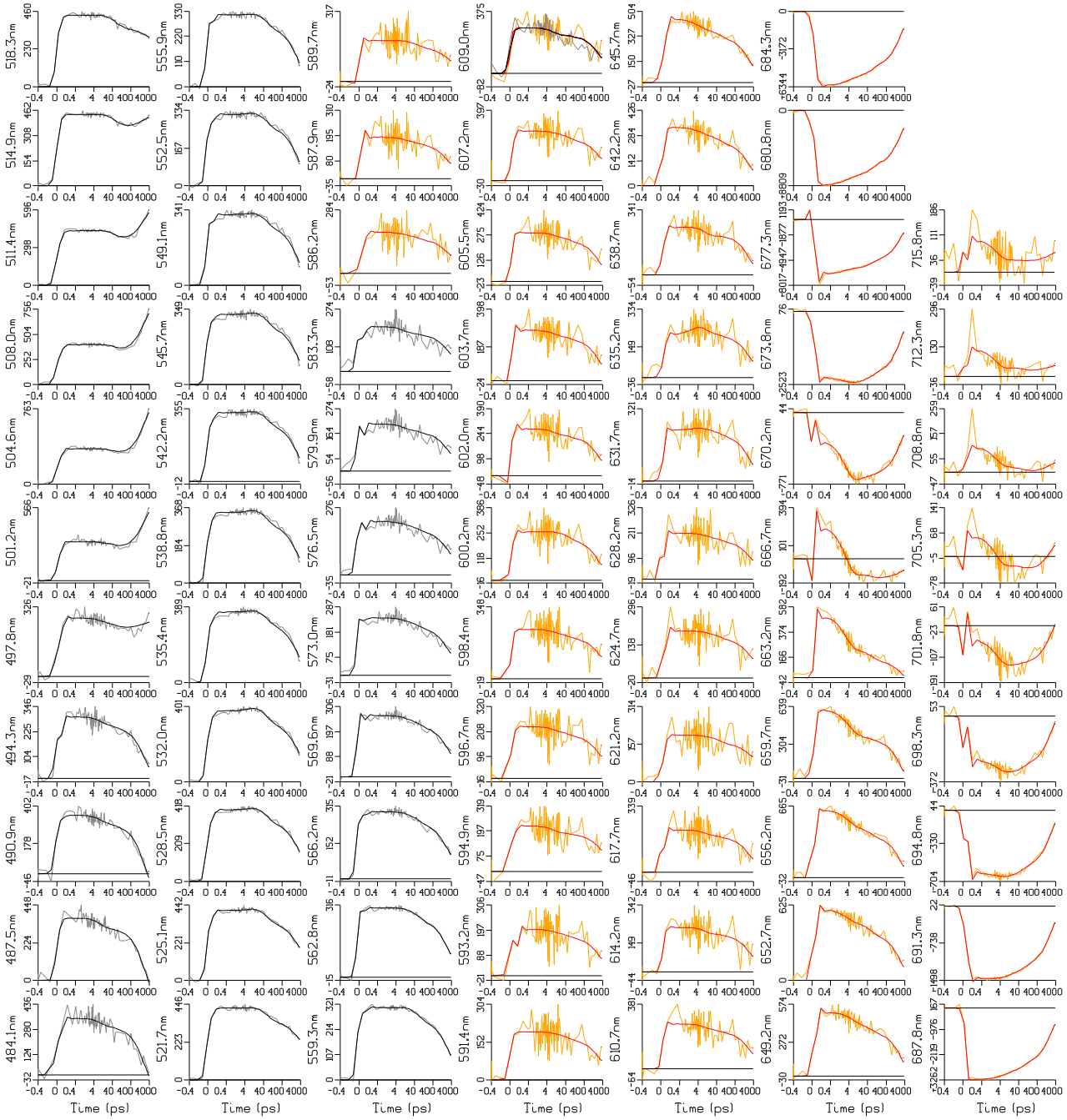

Figure S8. Transient absorption data and fitting: alternative equality constraints. Time traces of raw data (light colors, in μOD) and fit (dark colors) with the alternative equality constraints adopted in the Supplemental Information, Text S1 (ESA profile of all chlorophyll species forced to be equal). Wavelength is indicated in the ordinate label of each panel. Please note that the time scale is linear until 0.4 ps and logarithmic thereafter. Please note that each panel is scaled to its maximum and all the time zeroes (location of the maximum of the IRF) are chirp corrected.

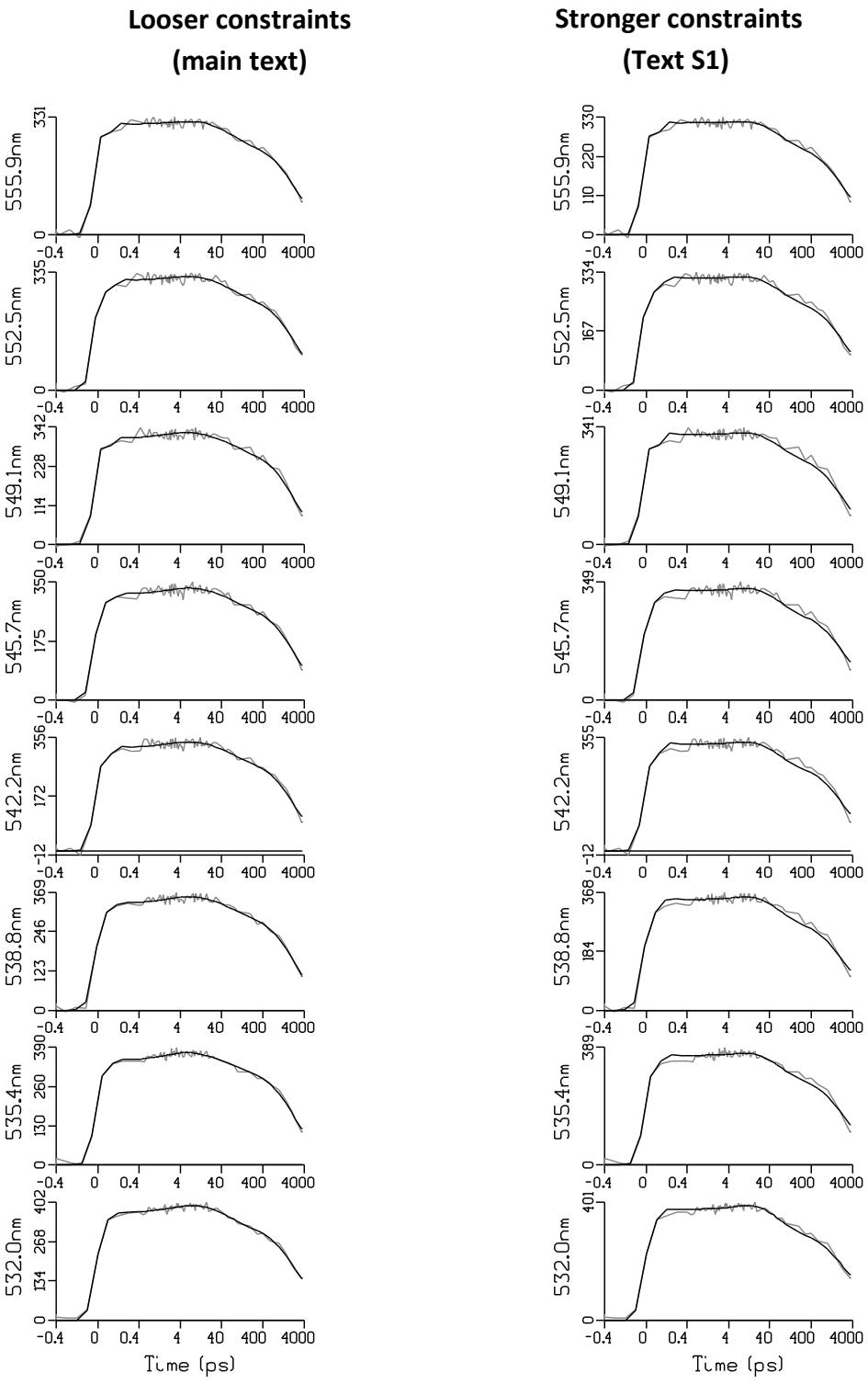

Figure S9. Transient absorption data and fitting: comparing different constraints. Zoom in of the experimental (light colors) and fit (dark color) traces between 532 nm and 556 nm, already shown in Figure S7 and S8. The left panel is referred to the set of equality constraints presented in the main text (leading to the best fitting). The right panel is referred to the alternative set of constraints presented in the Supplemental Information, Text S1.

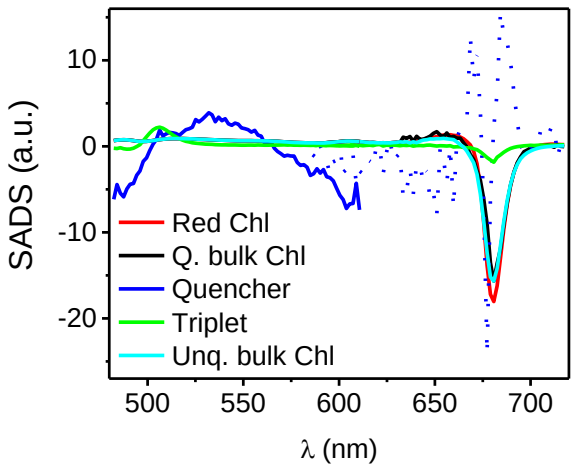

Figure S10. Alternative constraints on the target model (related to Figure 4A,B). Species associated decay spectra (SADS) of each compartment in the target model of Figure 4A in the main text, but using more restrictive equality constraints (all chlorophyll spectra equal at wavelengths shorter than 630 nm). The quencher spectrum in the Qy is depicted as a dotted line to allow better visualization of the chlorophyll spectra.

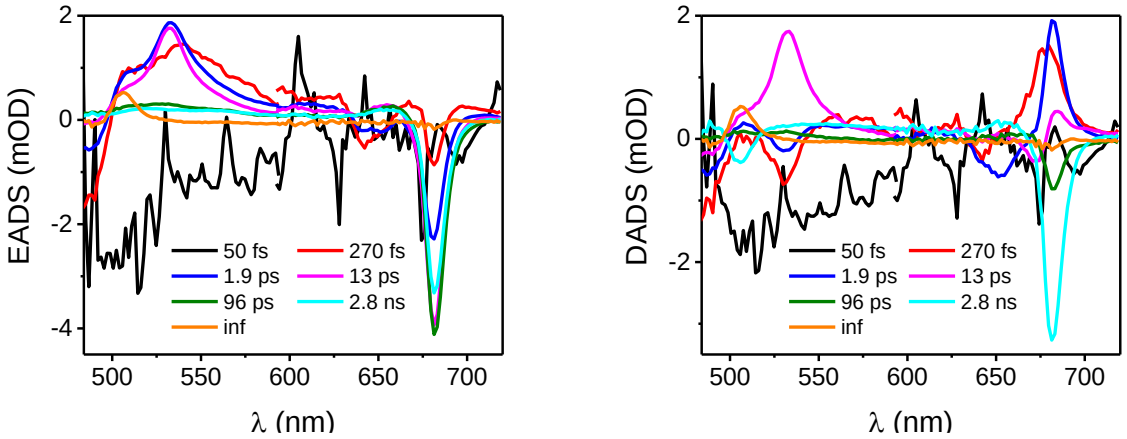

Figure S11. Transient absorption experiments upon carotenoid excitation. Evolution Associated Difference Spectra (EADS, left panel) and Decay Associated Difference Spectra (DADS, right panel) for the 489 nm excitation TA experiment on CP29 WT. The pump preferentially excites the carotenoid S_2 state, marked by a strong bleach in the high energy region (black EADS). This state quickly decays (the lifetime of 50 fs was fixed being at the limit of the experimental time resolution) to a lower energy carotenoid state (red EADS). At the same time, some bleach appears in the Qy region, implying that the carotenoid S_2 state transfers energy to the chlorophylls. The red EADS in the high energy region represents excited state absorption (ESA) from the vibrationally excited ("hot") S_1 state of carotenoids. Such state relaxes in about 0.3 ps to the S_1 state (blue EADS). At the same time, some extra bleach is formed in the Qy region and some energy transfer from chlorophyll b to chlorophyll a is also observed. Some further chlorophyll b/a equilibration takes place in 1.9 ps (blue to magenta EADS and blue DADS). The carotenoid S_1 state decays in 13 ps (magenta to green EADS, magenta DADS), without major changes in the Qy bleaching (magenta and green EADS nearly overlap in the Qy), meaning that the efficiency of energy transfer from the carotenoid S_1 state to the chlorophylls is low (if any). The remaining Qy bleach due to chlorophyll excited states relaxes with 96 ps and 2.8 ns time constants (stemming from quenched and unquenched CP29, green to cyan and cyan to orange EADS) and finally populates long-lived triplet states (orange EADS). These results are consistent with previous TA measurements on CP29[46]. The magenta DADS in the high energy region, peaking at 532 nm (lifetime of 13 ps), can be assumed to represent the spectrum of the carotenoid S_1 (Figure 4C in the main text). A previous study[46] demonstrated that this signal is originated from the carotenoid bound to the L2 site, i.e. violaxanthin (its shape and width are also compatible with that of the S_1 of violaxanthin in solution[47]). Such a signal might also contain smaller contributions from lutein and neoxanthin S_1 ESAs, which are expected to peak at even longer wavelengths (above 540-550 nm)[46,47]. Excitation at 509 nm results in very similar excited state dynamics, as well as direct carotenoid excitation in the mutants (data not shown).

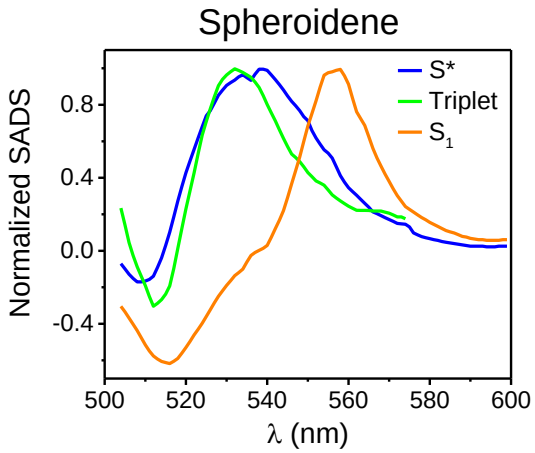

Figure S12. Carotenoid excited state spectra (related to Figure 4C). SADS for spheroidene S*, triplet and S_1 states from TA experiments on LH2 of *Rb. Sphaeroides*[49]. Similarly to what observed for the quencher SADS in CP29 (see Figure 4C in the main text), the S* spectrum exhibits a good overlap with the triplet spectrum and is significantly blue-shifted in comparison to the S_1 spectrum.

Text S2. Details about the wiggling feature in the Qy for the quencher spectrum

The quencher SADS shows a wiggling feature in the Qy region (blue SADS in Figure 4B, main text, and in Figure S10 for the alternative model). However, the signal to noise ratio in this spectral region is significantly worse than below 600 nm, where the carotenoid-resembling feature is present. A similar feature in the Qy was previously observed[22,55] and ascribed to coupling of Chlorophyll Qy transitions to the carotenoid excited state. However, we cannot exclude that such a signal arises from some minor slower energy transfer dynamics between chlorophylls which is not captured by the single equilibration step included in the model. It must be noted, however, that due to the very low concentration of the quencher and the large absolute signal in the Qy, the relative contribution of this signal to the Qy dynamics is practically negligible. On the other hand, the contribution of the quencher spectrum has a significant weight in the dynamics in the high energy region (480-570 nm).

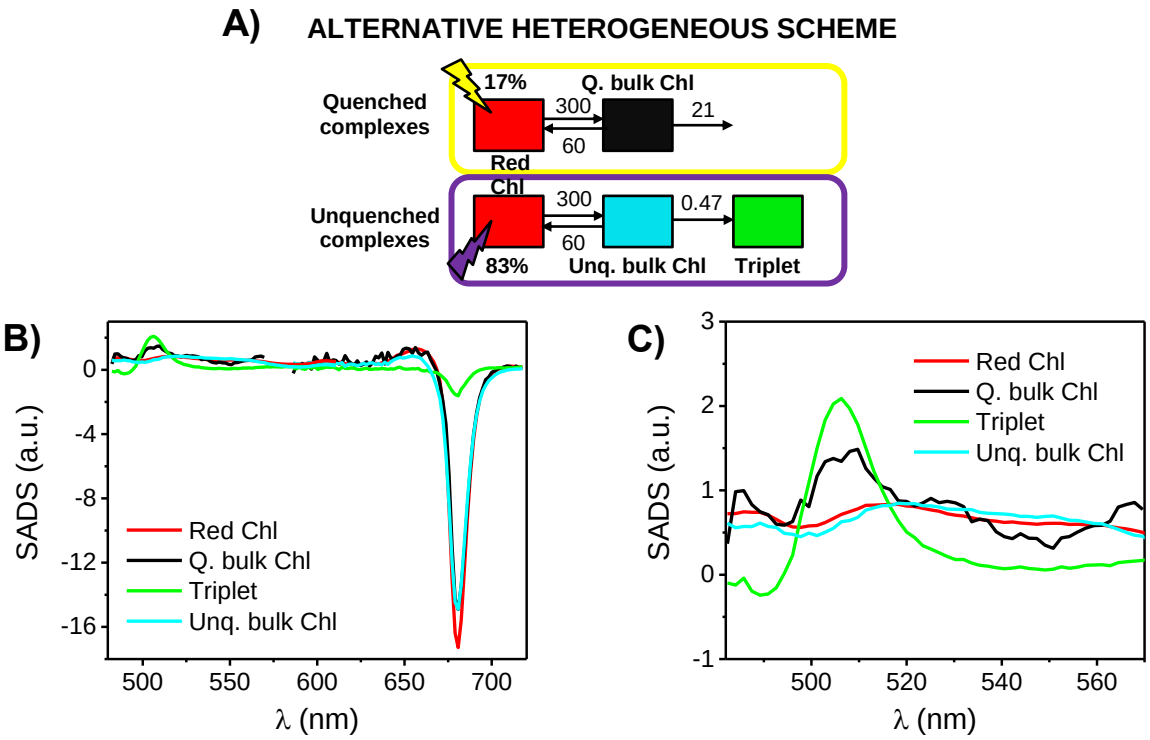

Figure S13. Alternative heterogeneous model without quencher (related to Figure 4). A) Alternative heterogeneous target scheme for the 682 nm excitation TA data of CP29 lacking the quencher compartment (i.e., quenched chlorophyll relaxes to the ground state directly). The model yields very similar kinetic rates as obtained from the heterogeneous kinetic model presented in the manuscript (i.e. with the addition of the quencher compartment, see Figure 4). B) SADS obtained from the scheme shown on top. C) expansion of ESA (excited state absorption) profiles of SADS shown in panel B). The quenched chlorophyll ESA profile (black SADS) exhibits a peak overlapping with the triplet spectrum and its shape is markedly different from that of the other chlorophyll species.

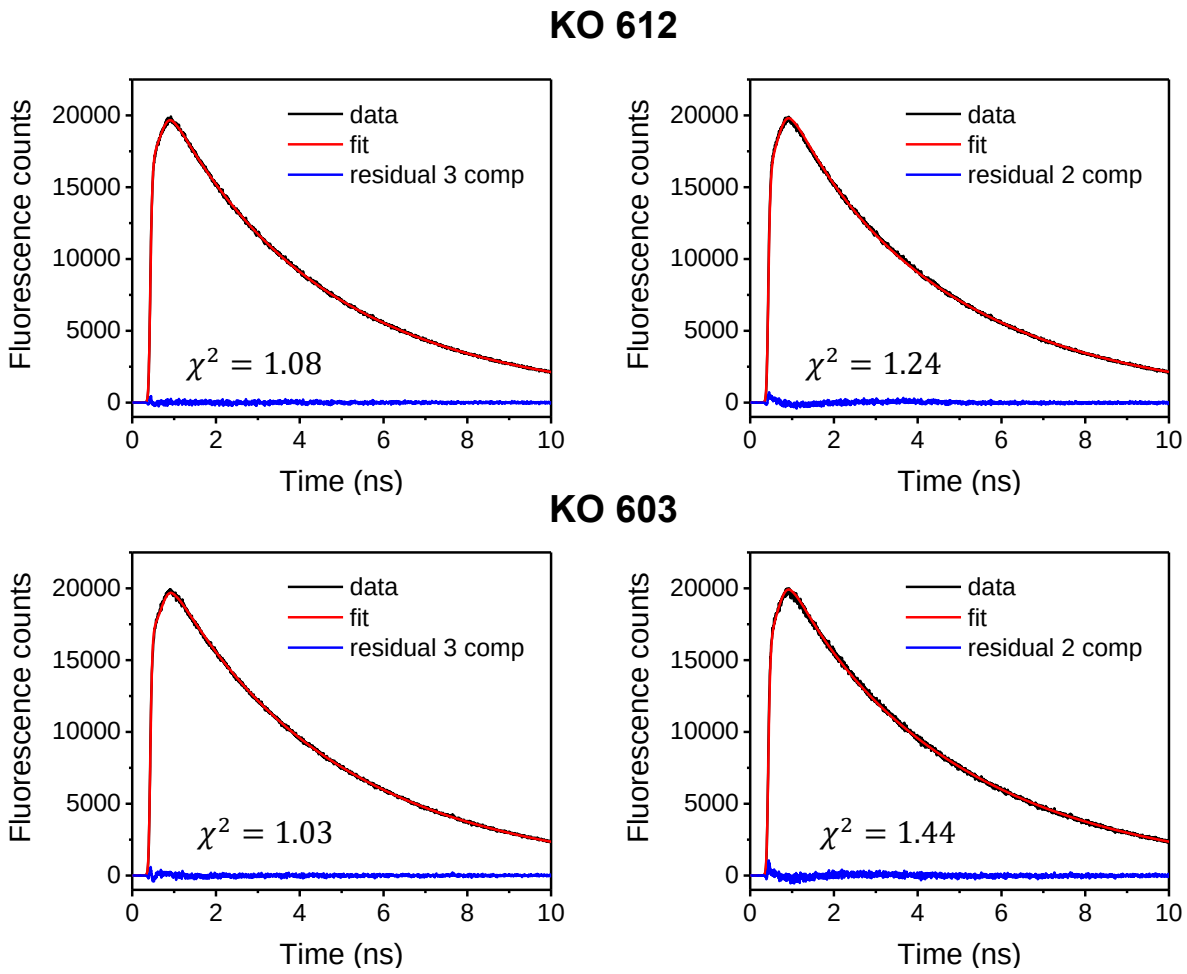

Figure S14. Time-resolved fluorescence experiments on CP29 mutants (related to Table 1). Measured (in black) and fitted (in red) fluorescence time traces at 680 nm for CP29 KO612 (top) and KO603 (bottom) upon 468 nm excitation. The difference between measured and fitted data (residuals) is displayed in blue. The left panels show the 3-component fitting presented in the main text with the relative χ^2. The right panels show a 2 component fitting for comparison. A 3-component fitting results in significantly lower χ^2 and less structured residuals, especially for CP29 KO603 (in a similar way as in the WT), implying that 3 components are necessary for a satisfactory fitting.

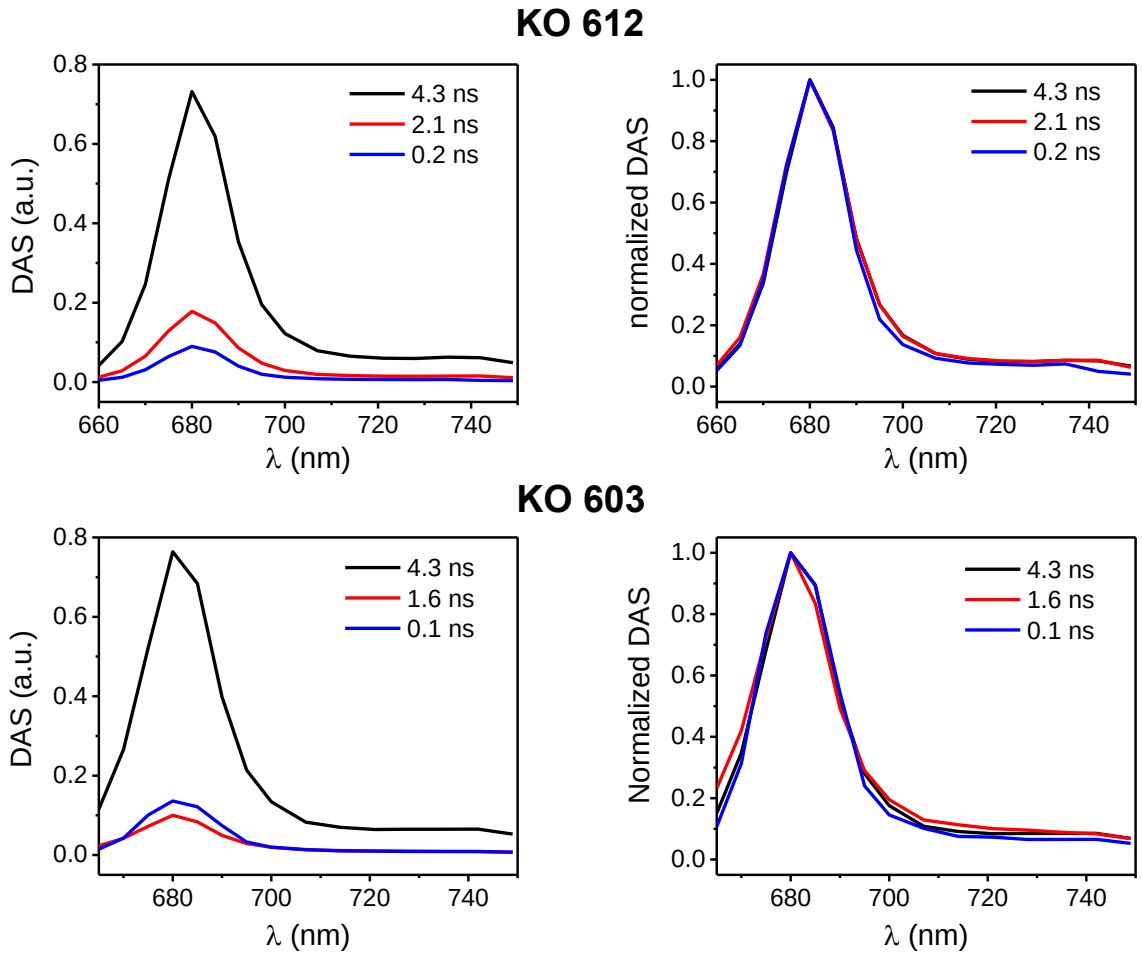

Figure S15. Fluorescence lifetime components of CP29 mutants (related to Figure 2). DAS (left) and normalized DAS (right) for time-resolved emission of CP29 KO612 (top) and KO603 (bottom) upon 468 excitation.

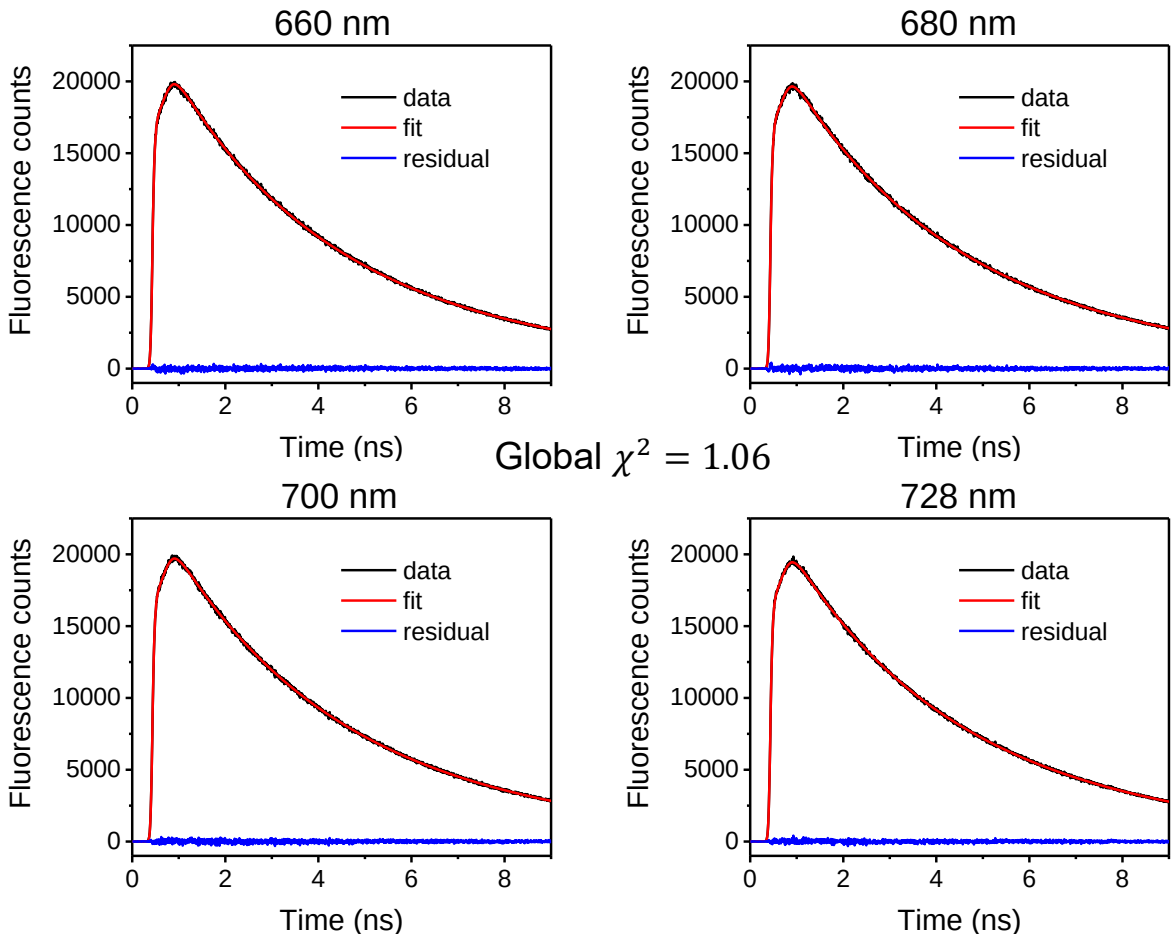

Figure S16. Time-resolved fluorescence experiments on CP29 KO612 at multiple wavelengths. Measured (in black) and fitted (in red) fluorescence time traces at selected wavelengths for CP29 KO612 upon 468 nm excitation. Residuals are displayed in blue.

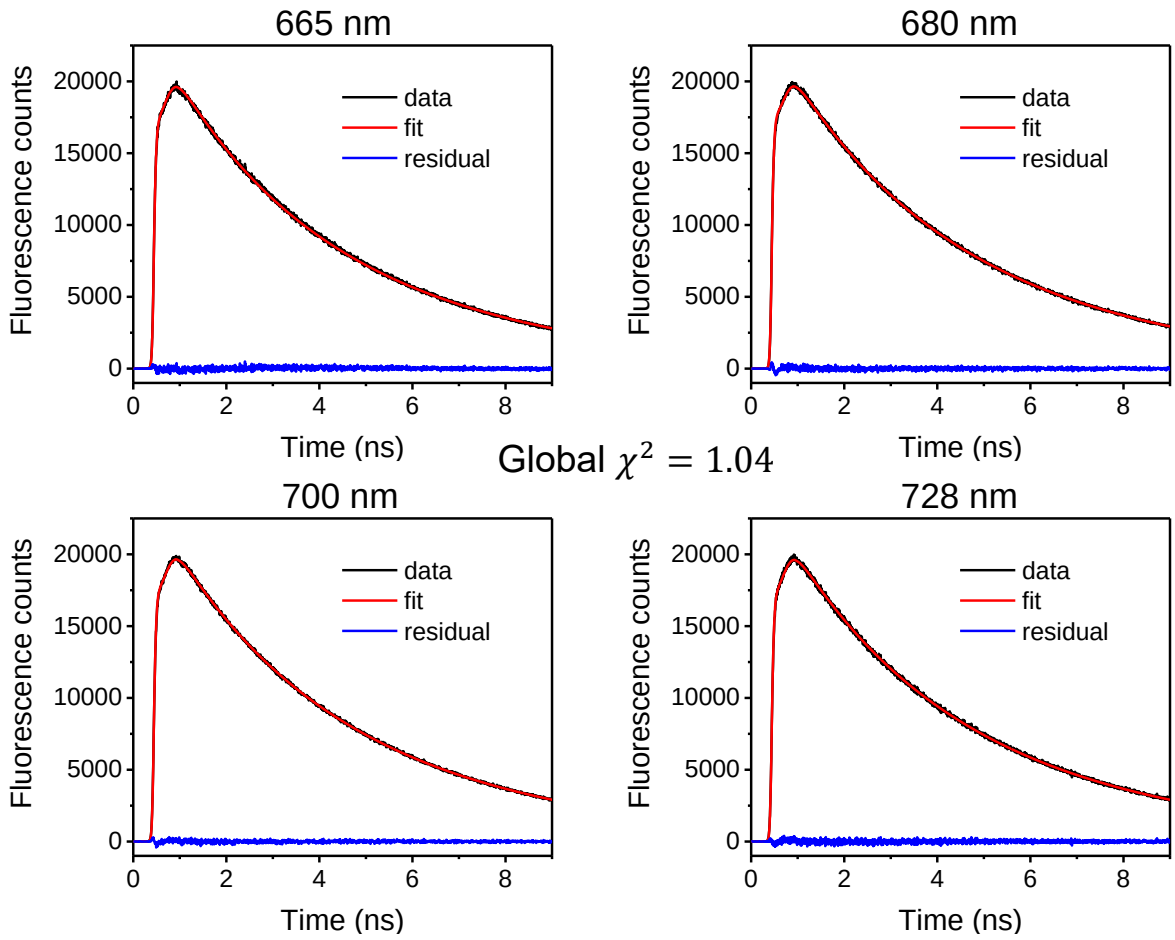

Figure S17. Time-resolved fluorescence experiments on CP29 KO603 at multiple wavelengths. Measured (in black) and fitted (in red) fluorescence time traces at selected wavelengths for CP29 KO603 upon 468 nm excitation. Residuals are displayed in blue.

Table S1. Lifetime components from transient absorption (related to Figure 5). Lifetime and amplitudes of fast and slow components from exponential fit of TA traces at 680 nm upon 672 nm excitation of CP29 WT and mutants (traces in Figure 5 of the manuscript).

	τ_{fast}	%	τ_{slow}	
CP29 WT	60 ps	16	2 ns	84
KO 612	-	-	2 ns	100
KO 603	60 ps	15	2 ns	85

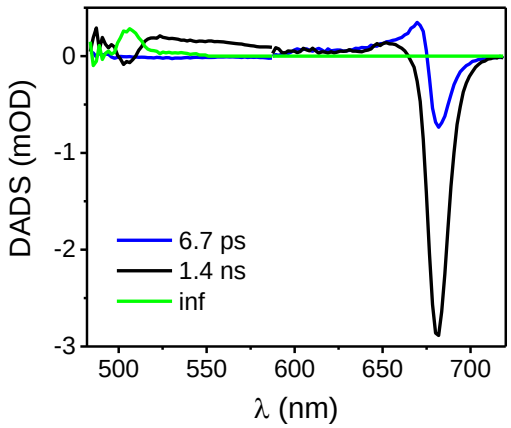

Figure S18. Transient absorption on CP29 KO612. DADS for CP29 KO612 upon 682 nm excitation. Uphill energy equilibration (blue DADS) is followed by chlorophyll excited state decay on a nanosecond timescale (black DADS, whose precise lifetime cannot be determined due to the limited time window of 1.5 ns), which results in triplet formation (green DADS). Due to the very limited fraction of quenched complexes, for CP29 KO612 only the predominant fraction of unquenched complexes is observed in the TA experiments (as can be appreciated in Figure 5 of the main text), whereas no strongly quenched component can be resolved (compare to Figure S5, where an extra DADS with 54 ps lifetime, in red, can be seen for CP29 WT).

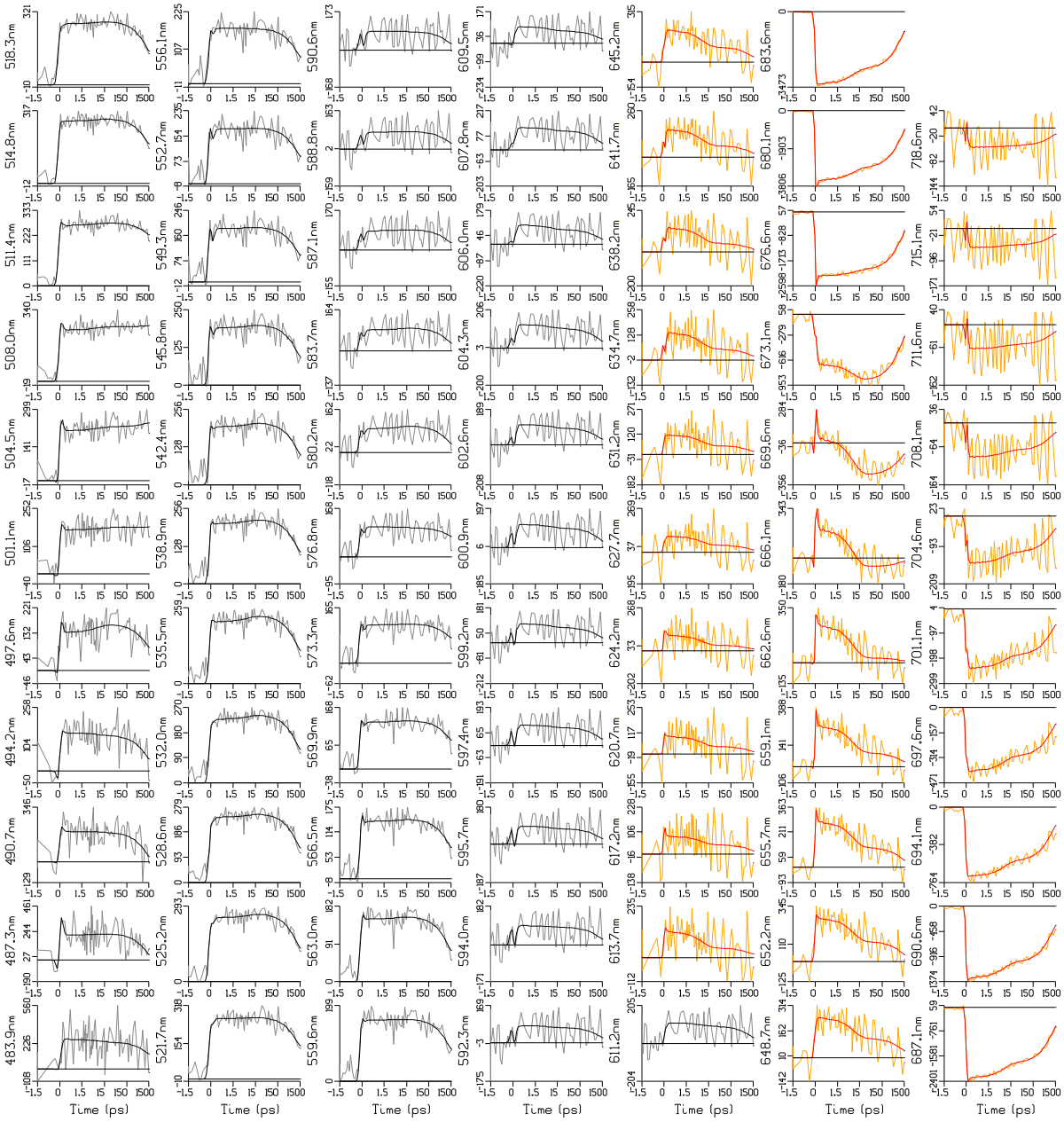

Figure S19. Transient absorption data and fitting for CP29 KO612. Time traces for CP29 KO612 upon 682 nm excitation of raw data (light colors, in µOD) and fit (dark colors) using the kinetic scheme with three DADS (Fig.S18). Wavelength is indicated in the ordinate label of each panel. Please note that the time scale is linear until 1.5 ps and logarithmic thereafter. Please note that each panel is scaled to its maximum.

Text S3. Power study

Transient absorption (TA) traces of CP29 WT measured at 680 nm upon different excitation pulse energies (with 672 nm excitation) and normalized at their minima are shown in Figure S19A. A fast excited state decay caused by annihilation starts to be discernible at excitation energies of 5 nJ per pulse or more. The onset for annihilation was therefore set to 5 nJ/pulse and all relevant measurement were performed below this threshold (3nJ/pulse for 682 nm). For direct carotenoid excitation higher energies could be used (5nJ/pulse at 489 nm and 10 nJ/pulse at 509 nm) due to the much lower absorption at 489 and 509 nm compared to that at 672 or 682 nm (Figure S4). Global analysis on the data matrices recorded at different excitation energies reveal that, above the annihilation threshold, an extra decay component appears, with a lifetime of 10-15 ps, whose amplitude increases with the pump power. Such component can be ascribed to annihilation. On the other hand, the relative amplitude of the 60 ps component, which is observed at all powers, is independent on the excitation energy (Figure S19B). This confirms that the 60 ps component represents a quenching process which is an intrinsic property of the protein ensemble. The lifetime of the power-dependent component is too long to be associated with singlet-singlet annihilation, since the energy equilibration in the complexes is completed on a shorter time scale[42] (around 5 ps). Moreover, the high repetition rate of the pump pulses (40/2 = 20 kHz) suggests that, at increasing powers, chlorophyll triplets can be accumulated on a fraction of the complexes. The interval between two consecutive pulses is indeed 50 µs, much shorter than the lifetime of chlorophyll triplets (on the order of 1 ms[44]), which can therefore accumulate in a significant amount of the monomers since chlorophyll to carotenoid triplet energy transfer is not 100% efficient. We therefore ascribe the observed power-dependent 10-15 ps component to singlet-triplet annihilation, taking place when an excitation is created in those complexes which previously accumulated a chlorophyll triplet. On top of that, singlet-singlet annihilation appears at high powers, resulting in additional signal loss on shorter timescales. The components related to singlet-triplet annihilation and quenched/unquenched complexes also exhibit different spectra in the Qy region, the former being significantly blue-shifted (Figure S19C and S19D). This suggests that the triplet-accumulating chlorophylls are not localized on the terminal emitter domains, consistent with carotenoid triplet quenching being more efficient on the low energy chlorophylls (including chlorophyll 612 and 603, which are also the closest to lutein and violaxanthin).

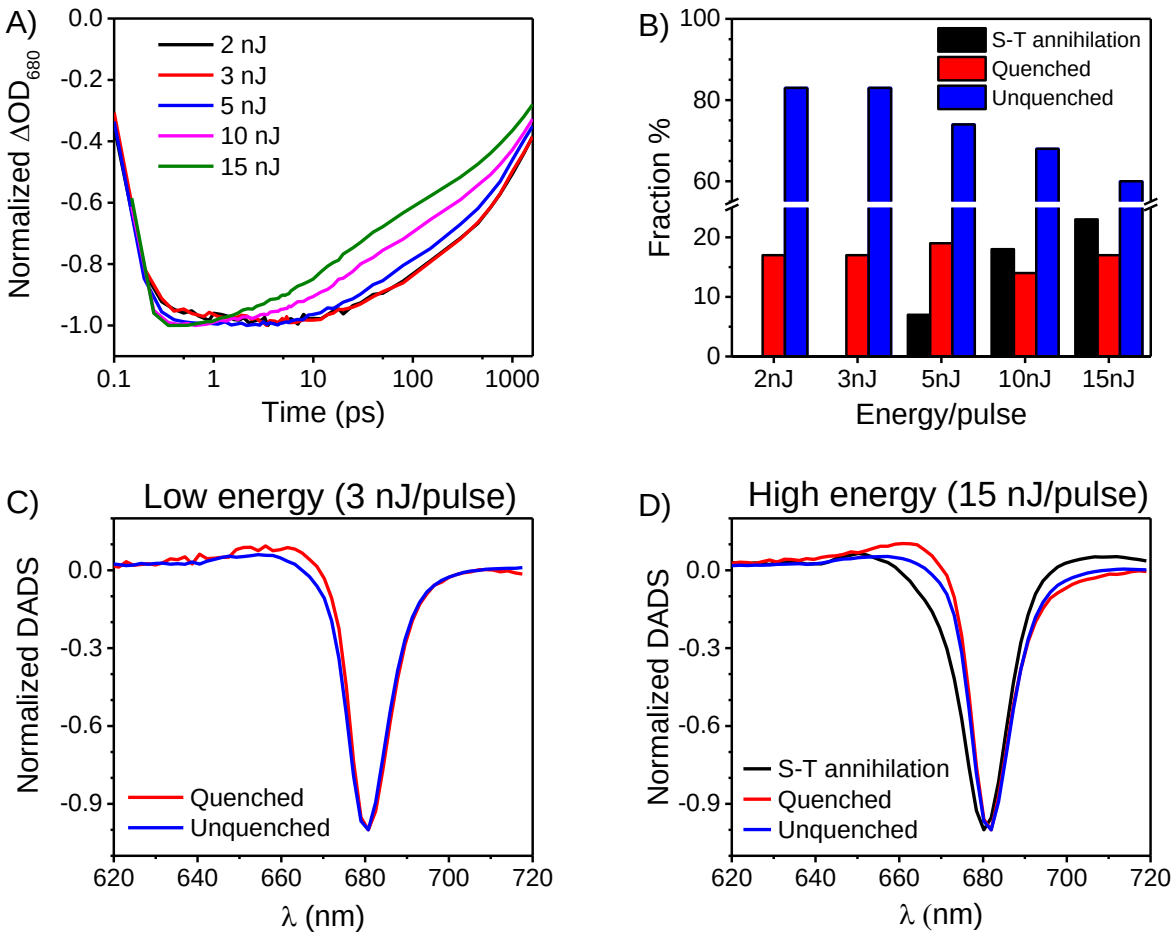

Figure S20. Power study. A) Normalized TA traces at 680 nm measured at different pulse energies (672 nm excitation) for CP29 WT. B) Amplitudes of the decay components obtained by globally analyzing TA data. The black, red and blue bars refer to the 10-15 ps, 60-70 ps and nanosecond components, which are ascribed to annihilation, quenched and unquenched complexes respectively. C,D) Normalized DADS for annihilation, quenched and unquenched components from TA data measured at 3 nJ/pulse (C) and 15 nJ/pulse (D) on CP29 WT.